Can Cathodoluminescence and Scanning Electron Acoustic Microscopy be Considered Complementary Techniques?

J. F. Bresse

France Telecom/CNET/DTD, jeanfrancois.bresse@cnet.francetelecom.fr

Follow this and additional works at: https://digitalcommons.usu.edu/microscopy

Part of the Biology Commons

Recommended Citation

Utah State University
MERRILL-CAZIER LIBRARY

CAN CATHODOLUMINESCENCE AND SCANNING ELECTRON ACOUSTIC MICROSCOPY BE CONSIDERED COMPLEMENTARY TECHNIQUES?

J.F. Bresse

France Telecom/CNET/DTD, Laboratoire de Bagneux,
196, avenue H.Ravera, B.P.107, 92225 Bagneux Cedex, France

Telephone no.: 33-1-4231 7243 / FAX no.: 33-1-4253 4930 / E-mail: jeanfrancois.bresse@cnet.francetelecom.fr

Abstract

Cathodoluminescence (CL) and Scanning Electron Acoustic Microscopy (SEAM) give complementary information on direct bandgap semiconductors when dopant impurities are introduced. CL deals with the electrical properties of the semiconductor and SEAM deals with the thermal and elastic properties and eventually with the piezoelectric properties in low doped III-V compounds. As function of the introduction of impurities for the doping of the semiconductor, the Near-Band-Edge (NBE) CL emission increases up to a maximum and decreases when the impurities are no longer introduced in electrically active sites, but create complexes giving rise to the appearance of a Deep Level (DL) emission. The increase of the SEAM signal is related to the reduction of the thermal conductivity as function of the introduction of the impurities when the lattice contribution of the thermal conductivity is preponderant versus the electronic contribution. For highly doped III-V compounds, variation in elastic properties and presence of strain in the layers may also be evoked to explain the increase of the SEAM signal. Examples of evolution of both CL and SEAM signals are given for introduced impurities, such as, Be, C, Si in GaAs. CL and SEAM are also compared from the point of view of probed depth and spatial resolution.

Key Words: Cathodoluminescence, Scanning Electron Acoustic Microscopy, semiconductor, carbon, beryllium, silicon, gallium arsenide, thermal properties, elastic properties, strain.

Introduction

Cathodoluminescence (CL) is known to give light emission in direct bandgap semiconductors at different wavelengths corresponding to the transitions through the energy levels due to impurities. The shallow levels of impurities situated in electrically active sites give the "Near Band Edge" (NBE) emission and the deep levels of the impurities introduced in non-active sites or forming complexes with the different atoms give the "Deep Level" (DL) emission. The NBE emission follows mainly the doping level until the introduction of impurities in non-active sites gives the DL signal.

Scanning Electron Acoustic Microscopy (SEAM) is based on the local thermal excitation of the sample and the detection of the acoustic waves generated in the heated zone due to the thermoelastic properties of the material [1, 5]. In piezoelectric materials, ionic crystals and low doped III-V compounds, piezoelectric coupling has been evoked to explain the results [11, 17].

Introduction of dopant impurities and lattice defects give rise to an increase of the SEAM signal which may be correlated to a reduction of the thermal conductivity. This has been shown in III-V compounds [3, 4]. We show here that the SEAM signal may also be correlated with the DL emission relating to the appearance of complexes during the incorporation of the impurities. The evolution of the three signals NBE, DL and SEAM may be explained by the incorporation of the dopant impurities either in electrically active sites or in non-active sites. In highly doped III-V compounds, such as, C and Be doped GaAs, we show that variations in elastic properties and strain state of the layer have to be taken into account to explain the increase of the SEAM signal.

Other combined use of CL and SEAM have been made to visualize N-type and semi-insulating III-V compounds [13], to visualize indium doped semi-insulating GaAs [14] and to visualize misfit dislocations in InGaAs/GaAs superlattices [18].

Cathodoluminescence, Principle, Physical Phenomena

Direct bandgap semiconductors can give a strong

luminescence under the electron excitation. When the electron beam loses its energy, it creates a great number of hole-electron pairs during its path. The mean energy for hole-electron pair creation, E_p, is nearly equal to 3 times the bandgap energy, E_G [10]. The number of created pairs per second, N_p, is given by [2]:

$$N_p = \left\{ \frac{I_b}{q} \cdot \frac{E_0}{E_p} \right\} \cdot \left\{ 1 - k\eta \right\} \tag{1}$$

where E_0 is the beam energy, I_b the beam intensity, q the electron charge, η the backscattering coefficient, k a correction factor.

The radiative recombination can give either an intrinsic luminescence with an energy equal to the bandgap, or an extrinsic luminescence related to the impurities and defects giving an energy level in the bandgap (either a shallow level or a deep level).

The generation rate for electrons and holes are equal:

$$G_n = G_p = \frac{N_p}{V} \quad \text{with} \quad V = \frac{\pi}{6} \cdot R_e^3 \tag{2}$$

where V is the interaction volume taken as a sphere tangent to the surface. The sphere diameter is equal to the electron penetration, R_e [8].

For a N-type semiconductor, only the holes in excess give the recombination. The mean density of carriers is:

$$\Delta p = G_p \tau_p \tag{3}$$

where τ_p is the total lifetime of the holes.

In order to determine the CL intensity, the continuity equation has to be solved. Its takes into account three phenomena: generation of minority carriers, their diffusion and their recombination. That gives the carrier density in each point of the semiconductor.

The number of generated photons, N_{ph}, depends on the carrier density and on the radiative phenomenon, governed by its radiative lifetime, τ_R.

In first approximation, we can write:

$$N_{ph} = \frac{1}{\tau R} \Delta p V = \frac{\tau_p}{\tau_R} \cdot N_p \tag{4}$$

The CL intensity must take into account the absorption of photons during their travel in the semiconductor, of the reflectance of the surface, R and of the angle of the cone, θ, giving the total reflection:

$$I_{CL} = \left\{ N_{ph} \exp(-\alpha d) \right\} \cdot \left\{ \frac{1 - \cos\theta}{2} \right\} \cdot \left\{ 1 - R \right\} \tag{5}$$

where $\theta = \arcsin(1/n)$, α is the absorption coefficient, d the mean emission depth, n the refraction index of the semiconductor.

Probed depth, spatial resolution

The probed depth corresponds to the maximum value of R_e and L, diffusion length of minority carriers.

$$L = (D\tau)^{1/2}$$

where D is the diffusion constant of carriers, τ lifetime of minority carriers.

The lateral spatial resolution, δ, is governed by 3 parameters: Φ_b beam spot size, R_e electron penetration, L diffusion length. By convoluting the three phenomena, we get:

$$\delta_{CL} = \left\{ \Phi_b^2 + R_e^2 + L^2 \right\}^{1/2} \tag{6}$$

SEAM principle, physical phenomena, signal amplitude

SEAM is based on a local excitation of the sample surface by a periodic electron excitation. In metals where the thermal phenomenon is the only contribution, the excitation causes a local periodic heating. The heat diffusion corresponding to this situation can be modeled by the development of a thermal wave which is so much damped that it does not propagate further than one wavelength (λ_T). The solution of the diffusion equation shows that the amplitude of the thermal wave is attenuated by a factor e after a propagation of one thermal diffusion length, μ, ($\mu = \lambda_T/2\pi$) expressed as:

$$\mu = \left\{ \frac{k'}{\pi f} \right\}^{1/2} \quad \text{with} \quad k' = \frac{k}{\rho C} \tag{7}$$

where k is the thermal conductivity, ρ the density, C the specific heat of the material, and f the operating frequency.

The local heating causes a dilatation of the sample giving a stress and a strain which is relaxed through acoustic waves generation. The acoustic wavelength, λ_a, is given by:

$$\lambda_a = \frac{v_s}{f} \tag{8}$$

Probed depth, spatial resolution

The probed depth is mainly governed by the thermal diffusion length, μ. When the detection is in phase with the excitation, the main part of the signal comes from the surface and when the detection is shifted in phase by $+ \pi/2$, the main part of the signal comes from a depth equal to $(\pi/4) \cdot \mu$.

The spatial resolution δ_{SEAM} is governed by three parameters: Φ_b beam spot size, R_e electron range, μ thermal diffusion length:

$$\delta_{SEAM} = \left\{ \Phi_b{}^2 + R^2 + \mu^2 \right\}^{1/2} \qquad (9)$$

Depending on the relative importance of these three parameters and the depth of the observed feature, D, one of these parameters will govern the spatial resolution. In Table 1, the different situations are shown and the main parameters governing the spatial resolution are given [16].

In most cases, the sample thickness is much less than the acoustic wavelength and the main contrast mechanism is not from acoustic origin. For example, at 1 MHz frequency, the acoustic wavelength is around 5 mm and most of our samples have a thickness of 500 μm or less.

For the other types of mechanism evoked to explain the signal generation, the main parameter governing the spatial resolution may be the minority carriers diffusion length in the case of the excess carrier mechanism or the electron range in the case of piezoelectric materials.

Signal amplitude

In the case of the thermal mechanism, theoretical expressions of the resultant stress for a specimen with a free surface have been given either in the one-dimensional case [15, 20] or in the three-dimensional case [7, 16].

In this case, the output of the transducer can be expressed as:

$$V_{acoust} = \left\{ R_{trans} \right\} \cdot \left\{ \frac{3 a_t B P_0}{(2 \pi f \rho C k)^{1/2}} \right\} \qquad (10)$$

with:

$$R_{trans} = \{g_{33} \cdot l_1\}/\{\pi b_1^2\}$$

where:

a_t	Linear coefficient of thermal expansion (K^{-1})
B	Bulk elastic modulus (N·cm^{-2})
P_0	Electron beam power (watt)
ρ	Density (g·cm^{-3})
C	Specific heat (J·g^{-1}·K^{-1})
k	Thermal conductivity (watt·cm^{-1}·K^{-1})
g_{33}	Transducer piezoelectric voltage constant (V·cm·N^{-1})
πb_1^2	Transducer-sample coupling area (cm^2)
l_1	Transducer thickness (cm)

In the other signal generation mechanisms, no expression have been given yet but the signal may depend on the piezoelectric stress constant and the elastic stiffness constant of the material for the piezoelectric coupling and on the minority carrier lifetime, permittivity and the elastic stiffness constant for the excess carrier mechanism [11].

Thermal conductivity in semiconductors

From the physics of solids, it is known that the thermal conductivity of semiconductors has two contributions given by the formula:

$$k = k_e + k_L \qquad (11)$$

k_e, electronic contribution, k_L, lattice contribution.

Electronic contribution

In semiconductors, one can evaluate this contribution by the formula:

$$k_e = \left\{ \frac{[(5/2) - s]k^2 \sigma T}{q^2} \right\} + \left\{ \frac{k^2 \sigma T (5 - 2s + E_G/kT)^2 np \mu_n \mu_p}{q^2 (n\mu_n + p\mu_p)^2} \right\} \qquad (12)$$

where k is the Boltzmann constant, σ the conductivity, q the electron charge, E_G the bandgap energy, T the temperature, n and p the electron and hole density, μ_n and μ_p the electron and hole mobility. s is given by the mean free time, τ_c, between carrier collisions which depends on the carrier energy E ($\tau_c = E^{-s}$). For a semiconductor with a spherical constant energy surface, such as GaAs, s = + 1/2 for phonon scattering, s = - 3/2 for ionized impurity scattering. For our calculations we choose s = - 3/2.

The electronic contribution has two terms: one related to the contribution of free electrons as in metals and the other due to carriers (minority and majority) which gives a mixed conduction. For most semiconductors, the second term may be quite large when $E_G >> kT$. This term decreases when the temperature increases. But in the second term, the product appears n x p = n_i^2, n_i being the intrinsic carrier concentration. This concentration is very low in GaAs ($1.7 \cdot 10^6$ cm^{-3} at T = 300 K). Thus, the second term is negligible.

Lattice contribution

The following expression is given for the lattice thermal conductivity [9]:

$$k_L = \left\{ (1/3)\rho C v_s l \right\} \qquad (13)$$

where C is the specific heat, v_s the average particle velocity and l the mean free path of particle between collisions. In solids, the particles are phonons and the phonon mean free path is determined by two processes: geometrical scattering and scattering with other phonons. When the anharmonic lattice interactions are not dominant, the mean free path is solely limited by the crystal imperfections [6].

Table 1. Spatial resolution and main contrast mechanism in SEAM.

Case	Spatial resolution	Main contrast mechanism
$\Phi_b/2 < R_e, \mu < D < \lambda_a$	λ_a	Acoustic
$\Phi_b/2 < R_e < D < \mu < \lambda_a$	μ	Thermoelastic
$\Phi_b/2 < D < \mu < R_e < \lambda_a$	μ	Thermoelastic and electronic
$\Phi_b/2 < D < R_e < \mu < \lambda_a$	R_e	Electronic and thermoelastic
$D < \Phi_b/2 < R_e < \mu < \lambda_a$	Φ_b	Electronic and thermoelastic

Table 2. Electronic contribution to the thermal conductivity for GaAs N-type and P-type for different doping levels.

Doping level (at·cm^{-3})	10^{16}	10^{17}	10^{18}	10^{19}	10^{20}
k_e N-type (W·cm^{-1}·K^{-1})	$8.9 \cdot 10^{-5}$	$6.9 \cdot 10^{-4}$	$4.0 \cdot 10^{-3}$	$1.7 \cdot 10^{-2}$	$7.1 \cdot 10^{-2}$
k_e P-type (W·cm^{-1}·K^{-1})	$4.6 \cdot 10^{-6}$	$3.8 \cdot 10^{-5}$	$2.3 \cdot 10^{-4}$	$1.2 \cdot 10^{-3}$	$5.5 \cdot 10^{-3}$

Table 3. Mean free path of phonons and lattice thermal conductivity in GaAs as a function of the impurity concentration.

Impurity number (at·cm^{-3})	10^{17}	10^{18}	10^{19}	10^{20}	10^{21}
l (nm)	13.3	6.2	2.88	1.33	0.62
k_L (W·cm^{-1}·K^{-1})	0.386	0.180	0.084	$3.86 \cdot 10^{-2}$	$1.80 \cdot 10^{-2}$

Table 4. Total thermal conductivity for N and P-type GaAs and the corresponding thermal diffusion length for different doping levels at a frequency of 250 kHz.

N_d (at·cm^{-3})	10^{17}	10^{18}	10^{19}	10^{20}
k (N-type) (W·cm^{-1}·K^{-1})	0.386	0.184	0.101	0.110
k (P-type) (W·cm^{-1}·K^{-1})	0.386	0.180	0.085	$4.41 \cdot 10^{-2}$
μ (N-type) (μm)	5.3	3.61	2.71	2.82
μ (P-type) (μm)	5.3	3.51	2.48	1.79

Thermal conductivity in GaAs as function of impurity concentration

We can evaluate the two contributions (electronic and lattice contribution) for a certain number of impurities which have been introduced in the semiconductor lattice. For the electronic contribution, we must take into account only the number of electrically active impurities in the lattice. For the lattice contribution, any impurity either in an electrically active site or in any lattice site or any type of defect in the lattice has to be taken into account. A lattice defect, such as an impurity complex, can also contribute to the reduction of the mean free path between collisions and then reduce the thermal conductivity.

For both N and P-type GaAs, n or p $<<$ n_i and the second term of eq. (12) is negligible and with s = -3/2:

$$k_e = 4k^2 \sigma T / q^2 \tag{14}$$

The conductivity σ can be evaluated from:

$$\sigma = q\mu_n n \quad \text{for N–type GaAs} \tag{15}$$

$$\sigma = q\mu_p p \quad \text{for P–type GaAs} \tag{16}$$

Knowing μ_n and μ_p, the electronic contribution k_e, can

be evaluated as a function of electron or hole density. Table 2 reports the results.

The experimental value of the thermal conductivity of GaAs is 0.46 $W \cdot cm^{-1} \cdot K^{-1}$ [6]. The effect of free carriers is nearly negligible except at very high electron concentration.

The specific heat of GaAs is 0.345 $J \cdot g^{-1} \cdot K^{-1}$ and the longitudinal sound velocity in GaAs(100) is $v_s = 4.75 \cdot 10^5$ $cm \cdot s^{-1}$. The phonon mean free path deduced for the intrinsic material is 83 nm. The effect of impurities or defects in the lattice causes a reduction of this phonon mean free path which may be evaluated in the following way: the volume of the unit cell of the GaAs lattice is given by:

$$V_u = a^3 \qquad (17)$$

where a is the lattice constant.

There are eight atoms in the unit cell. In the volume V_R, defined by a sphere of radius equal to the mean free path l, we find the same concentration of impurity atoms as in the bulk material, i.e.: N_I/N_a (N_I impurity atoms number per cm^{-3}, N_a lattice atoms number per cm^{-3}), thus:

$$\left\{ \frac{V_u}{8 V_R} \right\} = \left\{ \frac{N_I}{N_a} \right\} \qquad (18)$$

So, the mean distance between impurity atoms and the lattice conductivity can be evaluated as a function of the impurity concentration (see Table 3).

Table 4 gives for different doping levels, if all the impurities are electrically active, the total thermal conductivity for N and P-type GaAs and the corresponding thermal diffusion length at a frequency of 250 kHz.

Experimental Setup

The CL experiments have been performed in a JEOL 840 (JEOL, Tokyo, Japan) Scanning Electron Microscope equipped with a helium cooled stage and an ellipsoidal mirror for the light collection designed by Oxford Instruments (Witney, Oxon, England). The light is transferred via a light guide to a monochromator Jobin Yvon HR320 (ISA, Longjumeau, France) and filtered with a spectral resolution of 5 nm. The detection is made by a liquid nitrogen cooled Ge photodiode (North Coast, Santa Rosa, CA, USA). The overall spectral range for the detection is from 0.6 to 2.0 μm. The electron beam energy is adjusted in order to keep the electron penetration in the doped GaAs layer and the beam current is less than 1 nA, assuming low injection conditions. The experiments are made with the helium cooled stage. The estimated temperature of the sample is around 10K.

The SEAM experiments have been performed using a commercial system delivered by Cambridge Technology Ltd (Cambridge, England). The operating frequency can be varied from 10 kHz to 2 MHz. The samples are directly attached on the transducer itself by mixing a specific glue and Aquadag (Ladd Research Industries, Inc., PO Box 1005, Burlington, Vermont, 05402, USA). Samples are usually no greater than 5 x 5 mm. Since the conversion efficiency is low, especially for semiconductors, the operating parameters for the electron beam are usually: 10^{-6} Amp, 5-40 keV in order to get a signal greater than the electronic noise. For imaging an averaging (time constant 300 μsec) is done by a lock-in-amplifier. The frequency is usually 200 kHz and is adjusted in order to catch the resonance frequency of the assembly sample-glue-transducer. In order to compare the signal for samples of different doping levels, all the samples are cut and glued on the same transducer. The experiments are made at room temperature.

Evolution of CL and SEAM signals as function of the dopant impurity concentration

The samples studied are grown by molecular beam epitaxy (MBE). Several types of epitaxial doped layers are grown: 5 μm thick GaAs:Be layers on GaAs substrate with doping levels varying from $6.5 \cdot 10^{17}$ to $6.5 \cdot 10^{20}$ at·cm^{-3}, 1 μm thick GaAs:Si layers with doping levels from $1.0 \cdot 10^{17}$ to $6.3 \cdot 10^{18}$ at.cm^{-3} and 0.8 μm thick GaAs:C layers with doping levels varying from $7.0 \cdot 10^{17}$ to $4.3 \cdot 10^{19}$ at·cm^{-3}. All the given doping levels are measured by the Hall effect and correspond to electrically active impurity concentrations.

Constant beam energy and beam current are used for the experiments. The spot size is around 2.5 μm and the maximum electron range is 0.8 μm at 10 keV, 2.5 μm at 20 keV and 6.0 μm at 40 keV beam energy. The beam energy is adjusted in order to keep most of the electron penetration in the layer thickness. For the case of Be doped GaAs, it has been shown that it is possible to incorporate up to 10^{20} at·cm^{-3} in electrically active sites (acceptor type) with the following growth conditions: substrate temperature 600°C, V/III ratio of 15 [12]. The studied samples have a NBE emission wavelength varying from 836 nm (1.483 eV) to 866 nm (1.432 eV) with a peak width varying from 50 to 130 meV. They give a very small deep level emission (at around 1.35 μm, i.e. 0.92 eV), probably due to the absence of formation of Be complexes. Figure 1 reports the evolution of the NBE signal and the SEAM signal as function of the doping level. The evolution of the NBE signal represents the incorporation of Be in electrically active sites. The decrease of the NBE signal can be interpreted by the incorporation of Be in non-electrically
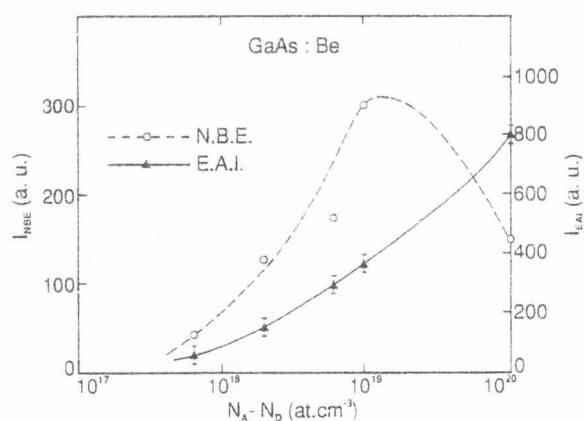
Figure 1. Evolution of the near-band-edge (NBE) emission in cathodoluminescence and the electron acoustic (EAI) signal for Be doped GaAs as function of the doping level (N_A-N_D).

---

active sites (interstitial sites, ...) creating defects in the lattice structure. These defects act as non-radiative centers decreasing the total lifetime of the carriers and causing the decrease of the NBE signal. The evolution of the SEAM signal is inverse of the NBE signal and follows the incorporation of Be.

For the case of C doped GaAs layers, we have studied the incorporation of C with a growth rate of 1 μm/hour (maximum cell temperature: 1870°C). The studied samples have a NBE emission wavelength varying from 838 nm (1.480 eV) to 862 nm (1.439 eV) with a peak width varying from 50 to 120 meV. As for the case of Be doped layers, C does not form complexes giving a detectable deep level emission. We have followed the NBE and the SEAM signal as function of the doping level (Fig. 2). The strong decrease of the NBE signal shows that the carbon does not incorporate in electrically active sites creating non-radiative centers, thus decreasing the total lifetime and the NBE signal. The incorporation of carbon in interstitial sites in the lattice may explain the strong evolution of the SEAM signal.

For the case of Si doped GaAs, we have studied the incorporation as function of the silicon cell temperature. The studied samples have a NBE emission wavelength varying from 867 nm (1.431 eV) to 818 nm (1.515 eV) with a peak width varying from 20 to 150 meV. The deep level emission has two peaks: one situated at 1.055 μm (1.175 eV) with a peak width of 250 meV and another around 1.7 μm (0.729 eV). Only the first one increases with the incorporation of Si. Figure 3 shows the evolution of two signals of cathodoluminescence: NBE and DL emissions, as well as the SEAM signal as a function of the net doping level. The NBE emission follows the incorporation in electrically active sites, as
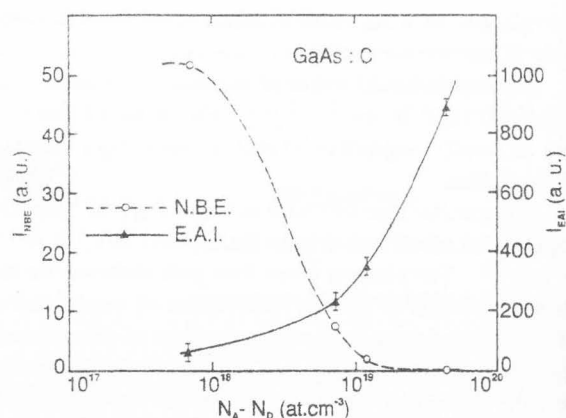

Figure 2. Evolution of the near-band-edge (NBE) emission in cathodoluminescence and the electron acoustic (EAI) signal for C doped GaAs as function of the doping level (N_A-N_D).
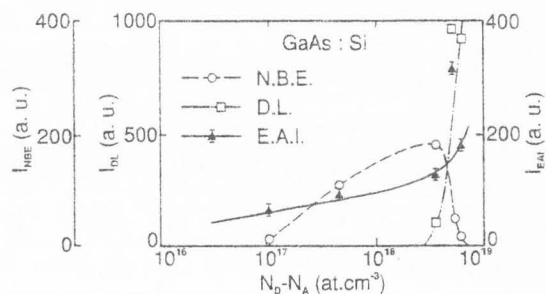

Figure 3. Evolution of the near-band-edge (NBE) emission, the deep level (DL) emission in cathodoluminescence and the electron acoustic (EAI) signal for Si doped GaAs as function of the net doping level (N_D-N_A).

---

acceptor and decreases after the appearance of non-radiative centers or deep levels. The deep level emission shows the appearance of radiative centers, mainly related to silicon complexes above a threshold doping level. The presence of deep levels and non-radiative centers has an effect on the total number of introduced impurities and thus reduce the thermal conductivity. This may explain the evolution of the SEAM signal.

We also report the results as function of the silicon cell temperature because as the cell temperature increases, the total number of introduced impurities increases but after a threshold the net doping level (N_D-N_A) decreases, due to the amphoteric character of silicon, and we observe a strong difference (Δ) between the net doping level and the total number of introduced impurities measured by SIMS.

Figure 4 shows the evolution of the net doping level (N_D-N_A), the NBE and DL emissions, the SEAM signal and Δ, the difference between the total introduced
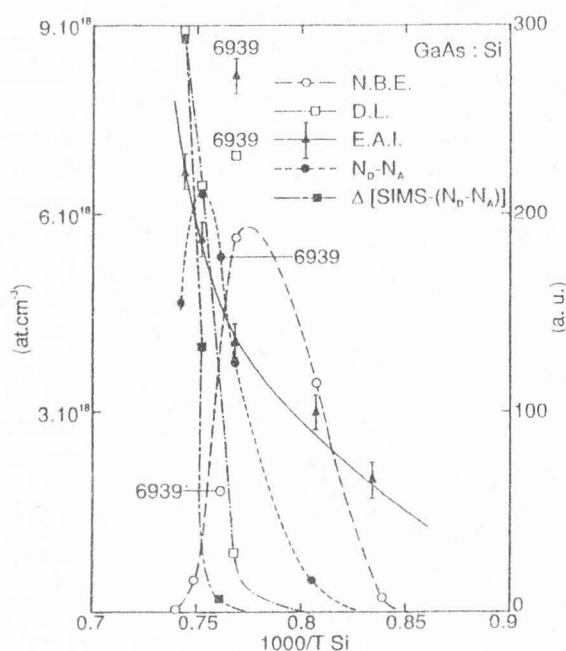
Figure 4. Evolution of the near-band-edge (NBE) emission, the deep level (DL) emission in cathodoluminescence, the electron acoustic (EAI) signal, the net doping level (N_D-N_A) and the difference Δ between the number of introduced impurities, measured by SIMS, and the net doping level for Si doped GaAs as function of the silicon cell temperature. The left vertical scale corresponds to the doping (N_D-N_A) and Δ, the right vertical scale corresponds to the NBE, DL and EAI signals.

---

impurities, measured by SIMS, and the net doping level as function of the inverse of the silicon cell temperature. A clear correlation exists between the evolution of the SEAM signal and the evolution of the DL emission and the total number of introduced impurities either in electrically active sites (acceptor or donor) or in complexes giving rise to the deep level emission. A good correlation exists also for the sample number 6939 (doping level $5.4 \cdot 10^{18}$ at·cm^{-3}) between the DL and the SEAM signals. This sample which has a stronger deep level signal exhibits a strong electron acoustic signal.

Discussion

The evolution of the SEAM signal can be explained by the variations of thermal and elastic properties of the semiconductor layer when the impurities are introduced.

In the case of Si doped GaAs layers, the evolution of the SEAM signal may be explained by the evolution of the thermal conductivity. For highest doping level $(4.7 \cdot 10^{18}$ cm$^{-3})$ the signal can be compared to the value

for the low doped level (10^{17} cm^{-3}). The ratio of the signals is about 3.5, corresponding to a decrease in conductivity of 12.5. Starting from the value given by the lattice conductivity at 10^{17} cm^{-3}, we get k = $3.06 \cdot 10^{-2}$ W·cm^{-1}·K^{-1}. At $4.7 \cdot 10^{18}$ cm^{-3}, the electronic contribution is k_e = $6.0 \cdot 10^{-4}$ W·cm^{-1}·K^{-1}. So we expect a lattice contribution of $3.00 \cdot 10^{-2}$ W·cm^{-1}·K^{-1} which gives a corresponding impurities and defects density of $2.0 \cdot 10^{20}$ at·cm^{-3}. The silicon content measured by SIMS is $1.4 \cdot 10^{19}$ at·cm^{-3}.

This value is lower because the thermal conductivity takes into account the total number of impurities and defects introduced in the lattice by the Si incorporation.

For Be or C doped GaAs layers, the evolution of the SEAM signal must take into account the combined evolution of the thermal and elastic properties of the layers to explain the increase of the signal. The change of boundary conditions due to the presence of strain in the layers must also be taken into account. It has been previously shown for photoacoustic experiments that the strain state of a layer may have aa strong influence on the signal [19]. It has been shown by SIMS experiments that the highly C or Be doped layers may contain several atomic percent of C or Be giving an alloy. The presence of an alloy has been observed by a shift in the CL NBE emission wavelength (12 nm for Be, 50 nm for C) and by a separate peak in X-ray diffraction corresponding to a lattice mismatch between the layer and the substrate. This lattice mismatch creates a strain in the layer. The introduction of up to 10^{21} at·cm^{-3} impurities with a doping level of 10^{20} at·cm^{-3} gives a total conductivity of $8.9 \cdot 10^{-3}$ W·cm^{-1}·K^{-1} and a decrease in thermal conductivity of 17.6 as compared to the low doped layer. This decrease is not sufficient to explain an increase of the SEAM signal of about a factor 16-18 between low and highly doped Be or C. The presence of an alloy may change the elastic bulk modulus but the strain in the layer may also have a strong influence on the signal.

Conclusion

In the study of semiconductors, CL and SEAM are complementary techniques. The different emissions of CL allow to detect the presence of dopants in electrically active sites by the NBE emission and the formation of complexes by the DL emission. The SEAM signal is directly related to the total number of impurities either in electrically active or non-active sites and the presence of non-radiative centers. In highly doped III-V compounds, such as, C or Be doped GaAs, variations in elastic properties and strain state of the layer have to be taken into account to explain the increase of the SEAM signal. When the CL yield is low, i.e. either in low doped or semi-insulating direct bandgap semiconductors or in highly doped direct bandgap semiconductors (when

the incorporation of impurities induces a lot of non-radiative centers or in indirect bandgap semiconductors), SEAM may be used with a good signal noise ratio. The origin of the SEAM signal is due to piezoelectric effects in low doped semiconductors and to the thermal and elastic properties in highly doped semiconductors.

Acknowledgments

References

[1] Brandis E, Rosencwaig A (1980) Thermal wave microscopy with electron beams. Appl Phys Lett **37**, 98-100.

[2] Bresse JF (1981) Quantitative investigations in semiconductor devices by electron beam induced current mode: A review. Scanning Electron Microsc **1981**; IV, 1487-1499.

[3] Bresse JF, Papadopoulo AC (1987) Be incorporation in heavily doped molecular beam epitaxy grown GaAs: Evidence of non-radiative behavior by cathodoluminescence and electron acoustic measurements. Appl Phys Lett **51**, 183-186.

[4] Bresse JF, Papadopoulo AC (1988) Evolution of the electron acoustic signal as function of doping level in III-V semiconductors. J Appl Phys **64**, 98-102.

[5] Cargill III GS (1980) Ultrasonic imaging in a scanning electron microscope. Nature **286**, 691-693.

[6] Holland MG (1965) In: Semiconductors and Semimetals, Vol. 2. Willardson RK, Beer AC (eds.). Academic Press, New York. pp. 3-5.

[7] Holstein WL (1985) Image formation in the electron thermoelastic acoustic microscopy. J Appl Phys **58**, 2008-2021.

[8] Kanaya K, Okoyama S (1972) Penetration and energy loss theory of electrons in solid targets. J Phys D **3**, 43-58.

[9] Kittel C (1986) Introduction to Solid State Physics. 6th Edition. Wiley, New York. pp. 115-124.

[10] Kobayashi T, Sugita T, Koyama M, Takayanagi S (1972) Performance of GaAs surface-barrier detectors made from high purity gallium arsenide. J Appl Phys **43**, 3302-3207.

[11] Kultscher N, Balk LJ (1986) Signal generation mechanisms in scanning electron acoustic microscopy. Scanning Electron Microsc **1986**; I: 33-43.

[12] Lievin JL, Alexandre F (1985) Ultra high doping levels of GaAs with beryllium by molecular beam epitaxy. Electron Lett **21**, 413-415.

[13] Mendez B, Piqueras J (1992) Application of scanning electron acoustic microscopy to the characterization of N-type and semi-insulating GaAs. Appl Phys Lett **60**, 1357-1359.

[14] Mendez B, Piqueras J (1993) Scanning electron acoustic microscopy of indium doped semi-insulating GaAs. Semicond Sci Technol **8**, 320-321.

[15] Opsal J, Rosencwaig A (1982) Thermal wave depth profiling: Theory. J Appl Phys **53**, 4240-4246.

[16] Qian M, Cantrell JH (1989) Signal generation in scanning electron acoustic microscopy. Mater Sci Eng **A122**, 57-64.

[17] Urchulutegui M, Piqueras J (1990) Signal generation mechanisms in scanning electron acoustic microscopy of ionic crystals. J Appl Phys **67**, 1-4.

[18] Urchulutegui M, Piqueras J, Salviati G, Lazzarini L (1993) Scanning electron acoustic microscopy of misfit dislocations in InGaAs/GaAs superlattices. J Phys D: Appl Phys **26**, 1537-1539.

[19] Von Gutfeld RJ, Melcher RL (1977) 20 MHz acoustic waves from pulsed thermoelastic expansions of constrained surfaces. Appl Phys Lett **30**, 257-259.

[20] White RM (1963) Generation of elastic waves by transient surface heating. J Appl Phys **34**, 3559-3567.

Discussion with Reviewers

G.S. Cargill III: Have you tried to look at DX-type deep levels by CL and/or SEAM, for example Sn- and Si-related DX levels in $Ga_{1-x}Al_xAs$, $x = 0.22 - 0.24$? In these systems at low temperature, $T < 20K$, electron emission for the DX centers, e.g. by IR illumination, produces persistent photoconductivity. X-ray diffraction measurements (G.S.Cargill III *et al.*, Phys Rev B **46**, 10078 (1992)) demonstrate that local expansion occurs when the DX centers are emptied. These might be an interesting system for CL and SEAM studies.

Author: We have done both CL and SEAM experiments at room temperature with $Ga_{1-x}Al_xAs$ samples, grown by MBE, with $x = 0.22-0.25$. In the first approach, we have seen the same behavior for the incorporation of Si in these samples, as in GaAs. With CL, we have seen a deep level situated 340 meV below the conduction band, strongly related to silicon. For the SEAM experiments, we have also seen the increase of the signal with the silicon incorporation. The effects you mention only appear at low temperature. We think that they might be visible in CL, however we have to consider the modification of the sample conductivity due to the fact that the traps are emptied by the electron beam ionization. The effects in SEAM might also be visible because the signal is very sensitive to the thermal expansion of the lattice. It could be preferable to study low doped samples where the thermal conductivity is higher at low temperature in order to reduce the increase of temperature due to the electron beam pulses and to stay in the metastability zone of the D-X centers.